JOURNAL OF MATERIALS SCIENCE **38** (2003) 3891 – 3902

An investigation of amorphous phase separation, leachability and surface area of an ionomer glass system and a sodium-boro-silicate glass system

A. RAFFERTY, R. HILL
Department of Materials Science and Technology, University of Limerick, Limerick, Ireland
E-mail: rafferta@tcd.ie

B. KELLEHER, T. O'DWYER
Department of Chemical and Environmental Life Sciences, University of Limerick, Limerick, Ireland

Glasses from a complex SiO_2-Al_2O_3-P_2O_5-CaO-CaF_2 glass series, known as 'ionomer glasses' were investigated. For comparison, a sodium-boro-silicate (s-b-s) glass system, which is known to undergo amorphous phase separation was also investigated. Scanning Electron Microscopy (SEM), Energy Dispersive X-ray Analysis (EDX) and BET surface area and pore distribution analysis were the principal analytical techniques used in this study. SEM analysis of the ionomer glass compositions revealed smooth spherical droplets of 2–15 nm while the background morphology appeared rough and speckled. A classic interconnected structure was observed for the s-b-s glass. EDX analysis of the s-b-s glass confirmed that the sodium-borate phase was removed by leaching with 0.3 M HNO_3, leaving behind a silica-rich structure. EDX analysis of ionomer glasses leached with 10% NaOH showed that the calcium and phosphate phases were being removed, although not to completion. For the base s-b-s glass a surface area of 8 $m^2\,g^{-1}$ was recorded. However, the base glass after extraction with 0.3 M HNO_3 of the sodium borate rich phase gave a BET surface area of 330 $m^2\,g^{-1}$ indicating that it had already undergone phase separation on quenching from the melt, giving rise to a fine scale interconnected structure. The leached s-b-s glasses exhibited type 4 adsorption/desorption isotherms characteristic of mesoporous materials. Glasses which had been heat treated at 580°C for 4 h exhibited a surface area of 62 $m^2\,g^{-1}$. This indicates that the as-quenched glass is already phase separated and that the phase separated microstructure is coarsening on heat treatment. A surface area of 4 $m^2\,g^{-1}$ was measured for the base ionomer glasses. After leaching with 10% NaOH this value rose 10-fold with a maximum surface area of 44.1 $m^2\,g^{-1}$ being recorded. The ionomer glasses also exhibited adsorption/desorption isotherms characteristic of mesoporous materials. © *2003 Kluwer Academic Publishers*

1. Introduction

Of great interest are microporous glasses suitable for performing separations such as industrial scale protein separation in the biotechnology and pharmaceutical industries. Because of its large surface area and controllable pore diameter, porous glass is a highly desirable filtering material. The surface of glass has a high affinity for certain molecules, thus making it possible to separate not only on the basis of molecular size, but also on molecular type [1]. Controlled-pore glasses have found wide application for size exclusion and adsorptive chromatography of proteins, nucleic acids, viruses, and high polymers [2]. The primary application is in permeation chromatography, where the chemical resistance and mechanical stability of porous glass significantly exceeds that of polymeric materials used for the same purpose. Because of the organophilic nature of porous glass, its internal surface can be modified with organo-functional silane coupling agents. The surface-treated controlled-pore glasses have found uses for the preparation of specialised diagnostic products and for the immobilisation of enzymes in fixed-bed reactors [2]. Advantages of porous glasses for filtration include rigidity, chemical inertness, high temperature capability, superior thermal shock resistance and controlled micro-porosity.

The existing microporous glasses used for protein separation are based on the sodium-boro-silicate system [3] where the mechanism of amorphous phase separation is exploited to give rise to interconnected silica rich and sodium borate phases. The sodium-borate phase is dissolved away in acid to leave a silica-rich microporous glass. While amorphous phase separation can occur in a large number of systems, in order to

0022–2461

produce a microporous material, certain requirements have to be fulfilled. Both phases must be interconnected and one phase must be highly soluble and the other relatively insoluble in a suitable reagent to allow selective leaching to occur. The degree of interconnectivity of the two glass phases is dependent on the nature of the phase-separation process. Nucleation and growth of the second phase gives, in the early stages, isolated spherical particles but when the volume fraction of this phase becomes sufficiently large, adjacent spheres may touch and partially coalesce resulting in an interconnected morphology [4]. In spinodal decomposition [5] an interconnected morphology develops in the early stages. The interconnected structure found in borosilicate glasses is widely believed to be due to a spinodal decomposition mechanism.

New microporous glass systems are constantly being sought to enable faster, more efficient separation of proteins using high pressure size exclusion and affinity chromatography techniques and lead to the industrial scale isolation of many new proteins. Biochemists would like to be able to remove proteins that become irreversibly bound to the microporous silica glass column, and to regenerate the microporous glass by washing with alkali, but alkalis dissolve the silica phase. Ordinarily a silicate glass can be made resistant to alkalis by incorporating alumina into the glass. But alumina hinders the amorphous phase separation process from taking place in the sodium-boro-silicate system [6]. Elmer *et al.* [7] of Corning Glass Works have tried to overcome this problem by moving to an aluminoborate system. Clark *et al.* [8] showed that glasses in the system Na_2O-Al_2O_3-B_2O_3 can be phase separated and leached yielding porous structures that are similar in porosity to porous high-silica structures obtained on leaching special soft alkali borosilicate glasses. Unfortunately, the porous alumina-rich structures could not be made in an unimpaired condition. Elmer *et al.* [9] then investigated glasses in the system Na_2O-Al_2O_3-B_2O_3-F and found that they can be converted to porous high-alumina structures by heat treating and leaching in hot dilute CH_3COOH solutions or H_2O. Chemical analyses of the leached samples showed that it was possible to extract a substantial amount of the non-aluminous constituents and produce a porous high-alumina structure, the final composition of which depends chiefly on glass composition and leaching conditions. Elmer *et al.* [9] used the BET method to measure surface areas of between 19 and 181 $m^2 g^{-1}$. Eguchi *et al.* [10] have invented a chemically durable porous glass of which the skeleton mainly comprises SiO_2-ZrO_2. They [10] claim to be able to produce a glass of which the skeleton is composed of alkali durable SiO_2-ZrO_2 components, which is not adversely affected through washing with alkali, so that it is feasible to completely remove gel substances from the glass.

The glasses that are used in making polyalkenoate dental cements are believed to undergo metastable phase separation in a similar fashion to those used for the existing microporous glasses and there is some evidence of a spinodal decomposition process [11]. Hill *et al.* [12] used scanning electron microscopy to study a SiO_2-Al_2O_3-CaO-CaF_2 based glass composition. After heating just past the glass transition, the glass exhibited an interconnected structure, suggesting that amorphous phase separation may be occurring by a spinodal decomposition mechanism. Clifford *et al.* [13] investigated a closely related glass composition that also contained calcium fluoride. Transmission electron microscopy using a carbon-platinum replica technique demonstrated evidence of amorphous phase separation giving rise to an interconnected structure. An acid leaching study [14] of an ionomer glass provided evidence suggesting the presence of an interconnected structure. The pattern of ion release implied that the glass consisted of two interconnected phases or a spinodal structure and not a dispersion of discrete droplets of one phase in another. Similarly, ionomer glass powders are commonly subjected to a process which is known as acid washing. This process was developed for improving cement setting times and decreasing cement water sensitivity. This technique can remove some of the calcium ions from the surface of the glass particles, thus delaying the initial set and increasing the working time and the setting characteristics. Jana *et al.* [15] have used what they refer to as acid etching, as a surface treatment to reduce the concentration of calcium and strontium ions in a glass-ceramic to enhance the working times of the cements for dental applications.

Barry *et al.* [16] observed phase separation of SiO_2-Al_2O_3-CaO-CaF_2 ionomer glasses into two phases; one of which was more susceptible to acid attack. Barry *et al.* [16] observed droplet interconnectivity for a number of the glasses they studied. An EDX study by Moisescu of an ionomer glass [17] showed it to consist of an alumina-silica rich phase, which is relatively resistant to acid attack and a calcium-phosphate rich phase, which is preferentially dissolved by acetic acid. It appears therefore, that there may be enough features present in these glasses to develop a new alumina-silica rich microporous glass that would be resistant to alkalis and therefore capable of regeneration by washing with alkali.

2. Experimental procedure

2.1. Glass synthesis

Ionomer glasses were synthesised containing the five components; SiO_2, Al_2O_3, P_2O_5, CaO and CaF_2. Table I shows the composition of the ionomer glasses studied along with their firing temperatures and calcium phosphate (Ca/P) ratios.

A fourth glass was also synthesised. This was a sodium-boro-silicate glass containing 51.5 wt% SiO_2, 40 wt% B_2O_3 and 8.5 wt% Na_2O which was produced

TABLE I Ionomer glass compositions studied in molar proportions

Glass	SiO_2	Al_2O_3	P_2O_5	CaO	CaF_2	Ca/P ratio	Melt temperature/°C
1	4.5	3	1.6	3	2	1.41	1420
2	4.5	3	1.4	3	2	1.61	1420
3	4.5	3	1.5	3.5	1.5	1.67	1430

in accordance with a composition chosen from a patent by Hammel *et al.* [1]. The ionomer glasses were prepared by melting appropriate amounts of the different glass reagents in lidded high density mullite crucibles (Zedmark Refractories, Earlsheaton, Dewsbury, UK) at 1420°C for 120 min. The resulting glass melts were then shock quenched directly into water to produce frit.

2.2. Glass leaching

A Labo Rota S300 Rotary Evaporator (Resona Technics, Switzerland) was used to conduct glass leaching experiments. A 1 litre florentine flask was used to hold the glass and the leachant. The set-up incorporated a condenser, which allowed leaching studies to be carried out over long time periods. The rotavapour bath contained water and was maintained at a constant temperature of 97°C. For the ionomer glasses a 10% NaOH leach was utilised. A 0.3 M HNO_3 etch was used for the sodium-boro-silicate glass, in accordance with the instructions given in the patent [1].

2.3. Brunauer-emmett-teller (BET) analysis

BET analysis was conducted on both base and leached ionomer and sodium-boro-silicate glass in order to determine the surface area and pore distribution of the glasses. Five point BET analyses were carried out in equal P/P_0 increments between 0.05 and 0.3. The pore size and pore volume distributions were also determined for some of the glasses on the basis of adsorption-desorption data. Isotherms were recorded at P/P_0's (∼30 steps) between 0 and 0.998 on the adsorption isotherm and from 0.998 to 0.4 on the desorption isotherm. A Micromeritics Gemini 2375 surface area analyser (Micromeritics Instrument Corporation, Norcross, U.S.A), was used for this analysis, using nitrogen as adsorbate. Each sample (∼50 mg) was outgassed under a vacuum for 2 h at 200°C before being analysed.

2.4. Scanning electron microscopy (SEM)

Samples were prepared by melting glass frit in alumina crucibles and casting onto a pre-heated sheet of steel. The glass sheet was then broken into pieces of glass of dimensions suitable for SEM analysis. The morphology of the samples was examined using an Hitachi S-4100 Field Emission Scanning Electron Microscope (Hitachi, Japan). The samples were fractured and etched for 10 s in 10% HNO_3. An SEM coating unit E5000 (Polaron Equipment Ltd., England) was used to gold coat the samples prior to examination.

2.5. Energy dispersive X-ray microanalysis (EDX)

Energy Dispersive X-ray (EDX) analysis (PGT, Peterborough, UK) was conducted on a number of glasses both prior to and after leaching to qualitatively assess the effect, if any, of leaching on the elemental glass composition.

3. Results and discussion

In two recent papers by these authors [18, 19], a powerful technique, high temperature DMTA was used to investigate the ionomer glasses and the sodium-boro-silicate glass system under investigation here. The findings of those studies supported the view that nucleation in both of these systems is via prior amorphous phase separation. In this study SEM is primarily used to investigate the APS behaviour with BET analysis being also employed as a novel alternative. Fig. 1 is an etched sample of the heat-treated sodium-boro-silicate glass and clearly shows a classical interconnected structure consisting of two mutually penetrating interconnected phases.

This structure closely resembles interconnected structures observed by authors such as Strnad [20], Haller [21], and Cahn [22, 23]. Of interest is the fact that prior to any heat-treatment this glass is optically clear, but that it turns opalescent in appearance following a heat-treatment. Previous DTA analyses [18] shows no evidence of a glass transition for the base glass but after a heat treatment a change in slope is observed at 395°C corresponding to a glass transition. It is speculated that the heat treatment for 4 h at 580°C must therefore result in coarsening of an already phase separated glass structure. The failure to detect a clear glass transition temperature in the initially quenched glass may be due to the size scale of phase separation being smaller than the size scale of the parts of the glass network associated with the glass transition. This view is supported to some degree by Mazurin [24] who postulates that in a rapidly chilled glass of given composition there is no framework of the high viscosity phase, and this framework is formed only during heat-treatment. At higher magnifications the pore structure can be more clearly seen and ranges from approximately 10 nm in narrow sections up to 300 nm in the wider sections. See Fig. 2.

Surface area is the product of the number of molecules in a completed monolayer times the effective cross-sectional area of an adsorbate molecule. There are many theories [25] for surface area calculation but the one most commonly used is that of Brunauer, Emmet and Teller also known as the BET method. Leaching experiments and BET analyses were conducted in an attempt to learn more about the phase separation process and to determine surface area measurements and pore size distributions for the sodium-boro-silicate system. A 0.3 M HNO_3 etch was used for the sodium-boro-silicate glass, in accordance with the instructions given in the patent [1]. The leaching stage involved an 8 h water leach followed by a 6 h acid leach and finally a 4 h water rinse. Table II details the leaching treatments that were used for the sodium-boro-silicate glass system and the surface area measurements recorded.

From Table II we see that the base glass yielded an average surface area of 8.5 $m^2 g^{-1}$. A sample of the glass, which had been heat-treated for 4 h at 580°C and then leached, yielded an average surface area of 62 $m^2 g^{-1}$. Leaching had the effect of removing the sodium-borate-rich phase, leaving a porous silica-rich structure and resulting in an approximately 7-fold increase in surface area over the base glass. The sample

TABLE II Leaching conditions and surface area measurements for the sodium-boro-silicate glass

Sodium-boro-silicate glass	Heat treatment	Distilled water leach	0.3 M HNO_3 leach	Distilled water rinse	Surface area ($m^2 g^{-1}$)
A1 run 1	None	None	None	None	8.7
A1 run 2	||	||	||	||	8.4
A2 run 1	240 mins@580°C	8 h	6 h	4 h	61.9
A2 run 2	||	||	||	||	62.5
A3 run 1	None	8 h	6 h	4 h	330.9
A3 run 2	||	||	||	||	336.4

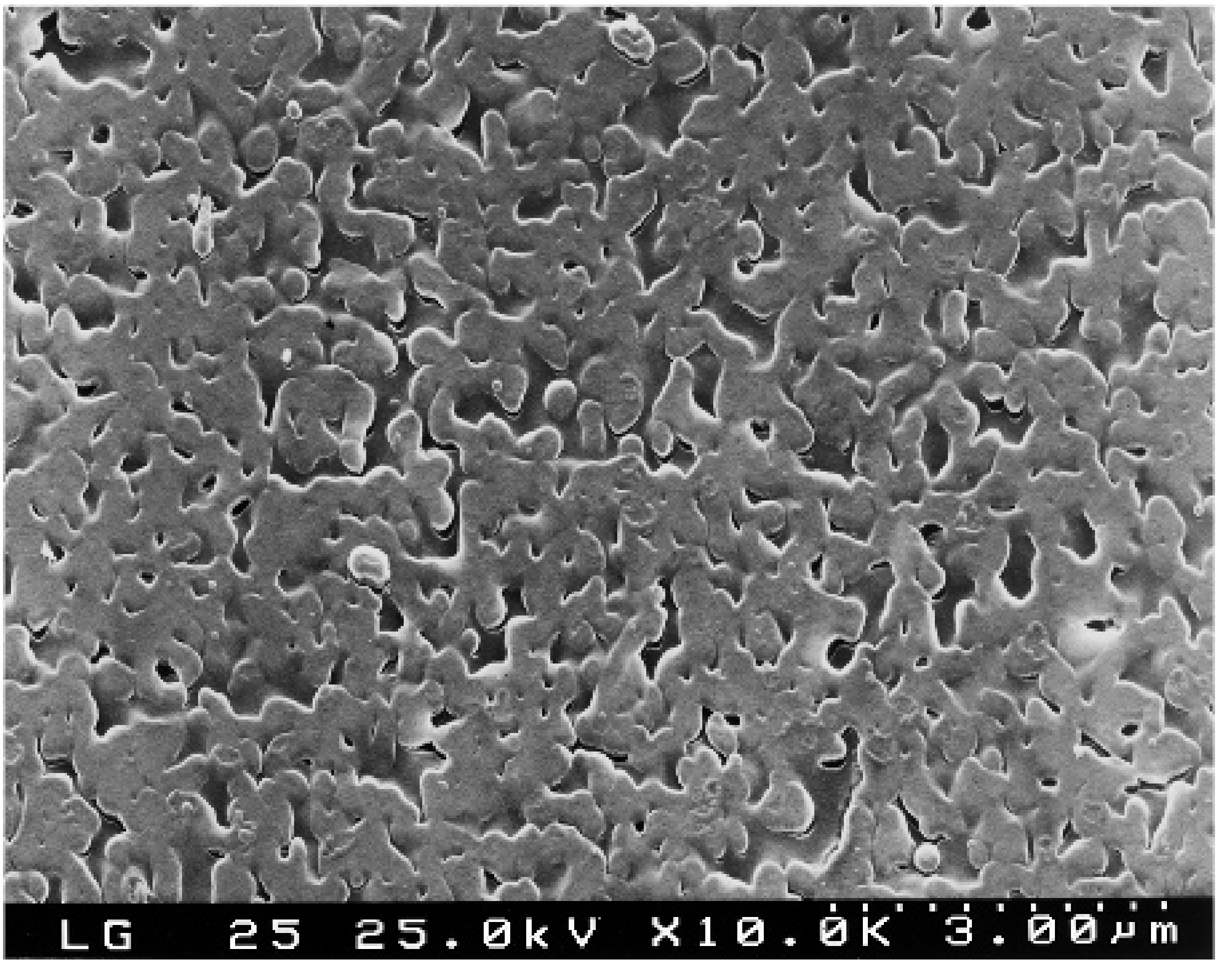

Figure 1 SEM of sodium-boro-silicate glass, heat-treated for 240 min at 580°C.

of the base glass which was then leached without any prior heat-treatment yielded an average surface area of 334 $m^2 g^{-1}$. This somewhat anomalous result indicates that the glass had phase separated on a very fine scale on pouring from the melt and confirms the earlier speculation that the heat treatment for 4 h at 580°C resulted in a coarsening of an already phase separated glass structure. This corresponds with previous DTA/TGA findings by these authors [18] where a glass transition was only evident for the heat-treated glass and not for the base glass. Leaching again removes the sodium-borate phase, but due to higher volume fraction of smaller size pore network, a much higher surface area is recorded. BET pore size distribution analysis was conducted on the base glass, sample Al. As expected, however, it was pore-free and therefore no isotherm or pore size distribution could be generated. An adsorption-desorption isotherm of sample A2 was generated however and this is shown in Fig. 3.

Brunauer, Deming, Deming and Teller [26], based upon an extensive literature survey, found that all adsorption isotherms fit into one of five types. The isotherm in Fig. 6 is characteristic of a Type 4 isotherm. A characteristic of Type 4 isotherms is the hysterisis loop. In this case the hysteresis is observed at high relative pressures for P/P_0 values of >0.6. Type 4 isotherms occur on porous adsorbents possessing pores in the radius range of approximately 15–1000 Å. The slope increase at higher elevated pressures indicates an increased uptake of adsorbate as the pores are being filled. The lower branch of the loop represents measurements obtained by progressive addition of gas to the system, and the upper branch by progressive withdrawal. This part of the isotherm is used for pore size distribution evaluation. The pore distribution, which was generated for sample A2 is shown in Fig. 4.

Pore systems of solids are of many different kinds but are generally categorised into several size ranges.

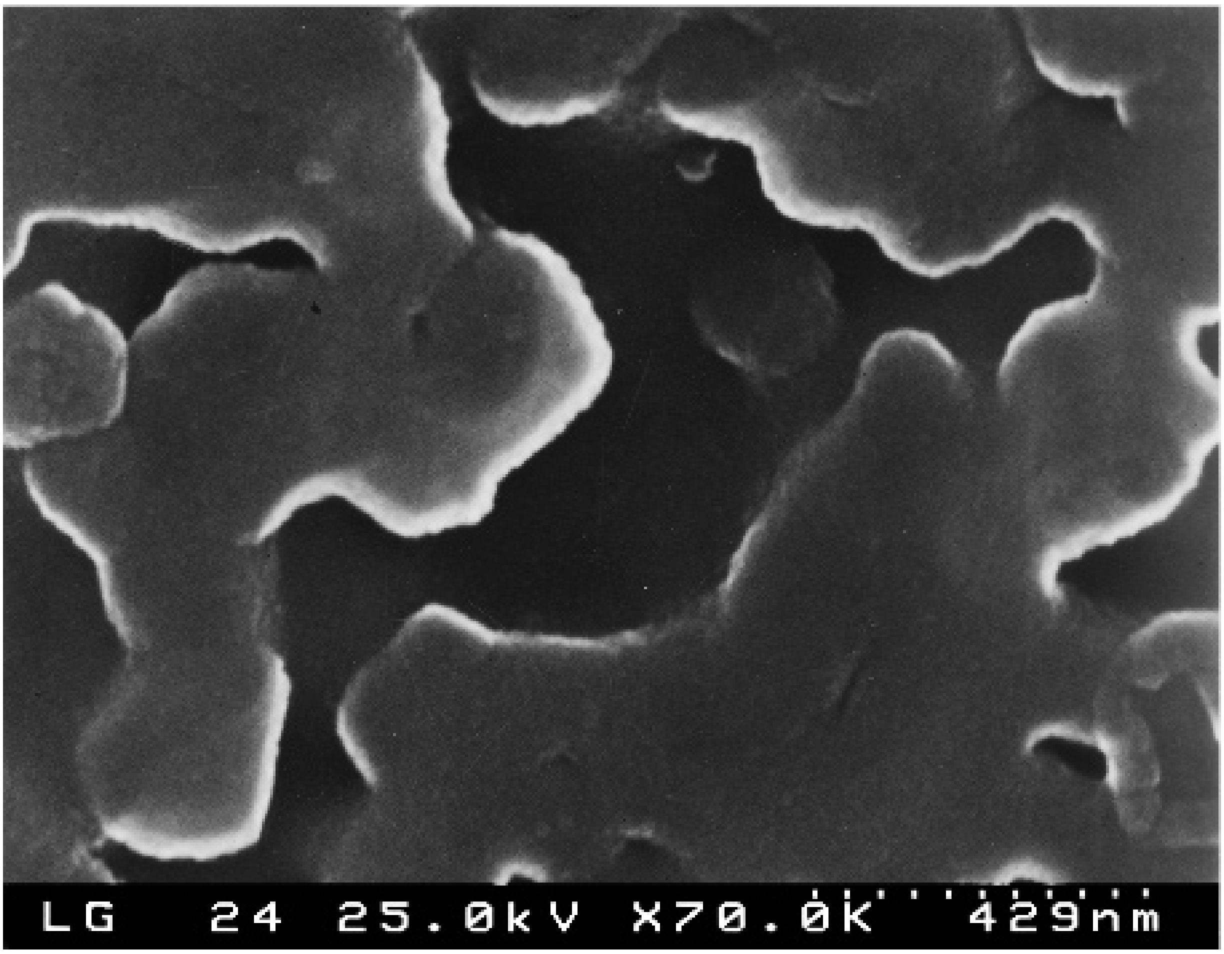

Figure 2 SEM of sodium-boro-silicate glass pore structure, heat-treated for 240 min at 580°C.

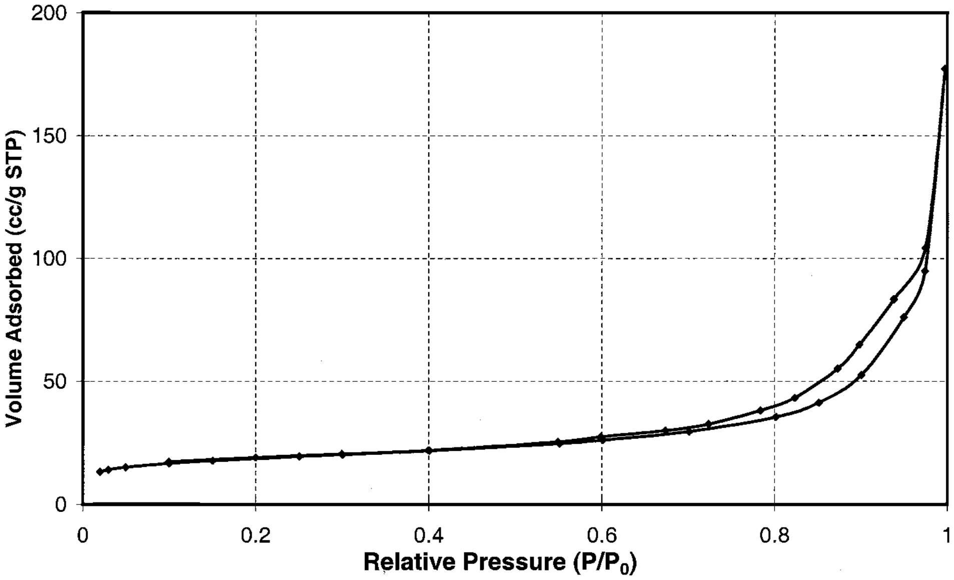

Figure 3 Adsorption-desorption isotherm for sample A2.

An accepted classification procedure originally proposed by Dubinin [27] and now officially adopted by the International Union of Pure and Applied Chemistry defines macropores as being >500 Å, mesopores as being 20–500 Å and micropores as being <20 Å. According to this classification the pores under discussion here should be classified as mesopores. Each of the size ranges correspond to characteristic adsorption effects as manifested in the isotherm. In mesopores, capillary condensation, with its characteristic hysteresis loop, takes place. Capillary condensation occurs in the pores of the material and is due to the favourable energy situation inside a pore which will allow a gas to condense into the pore under relative pressure conditions which would not normally allow this to happen on a non-porous surface.

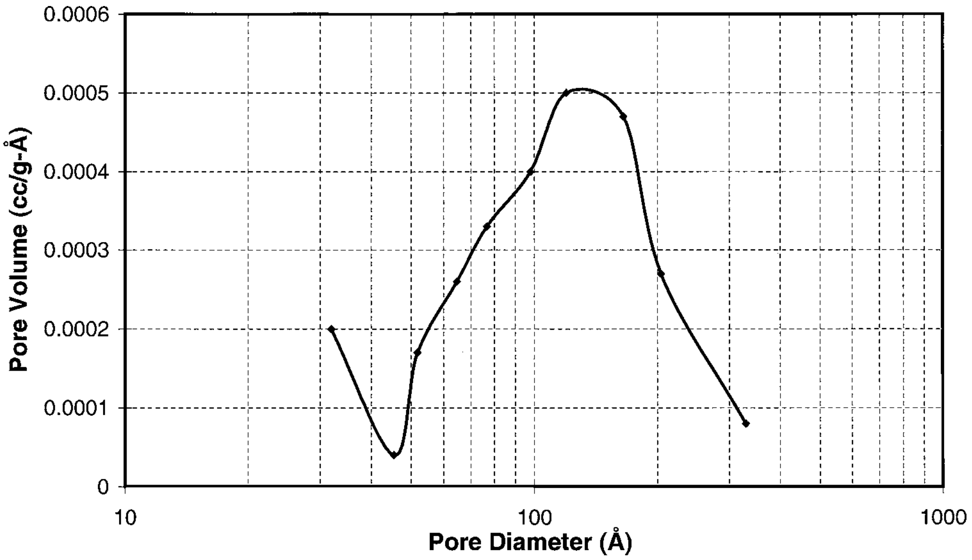

Figure 4 Pore distribution for sample A2.

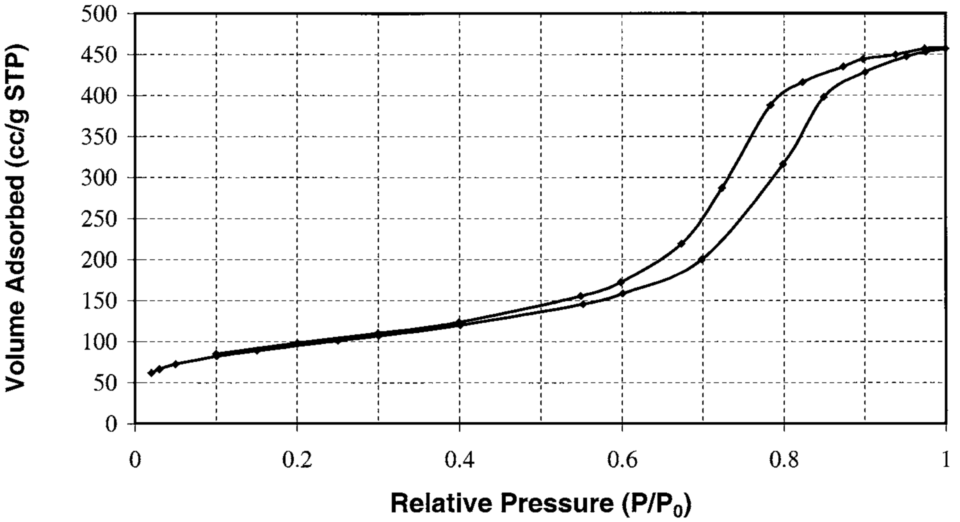

Figure 5 Adsorption-desorption isotherm for sample A3.

BET pore size distribution of sample A3 was carried out and again showed a type 4 isotherm but with hysteresis occurring at lower relative pressures (>0.4) than for sample A2, indicative of smaller pores. The volume adsorbed is approximately six times that of sample A2, indicating the greater number of pores present. See Fig. 5.

According to Storck *et al.* [28], type 4 isotherms are typical of mesoporous materials, while the increase in adsorbed volume at higher P/P_0 is caused by capillary condensation below the expected condensation pressure of the adsorbate. The findings for sample A3 add weight to the theory that the glass had phase separated on pouring from the melt on a very fine scale, resulting in mesopores on the lower end of the size scale.

A pore distribution for sample A3 showed a narrow pore range of approximately 4 to 11 nm. See Fig. 6.

The higher pore volume and smaller pore sizes observed for Sample A3 explain why a much higher surface area value was recorded. The larger pore sizes observed for sample A2 are as a result of the heat treatment, which coarsens the phase separated structure thus leading to a reduction in surface area after leaching.

EDX analysis of sample A1 exhibited a large peak for silicon along with a large oxygen peak, and a smaller sodium peak. See Fig. 7a. The EDX system was incapable of detecting boron. After leaching, (Sample A2), EDX analysis was repeated and only a minor oxygen peak and a large silicon peak remained. This is to be expected, following the leaching out of the sodium-borate rich phase. See Fig. 7b.

Scanning electron microscopy of the ionomer glasses was conducted to find evidence for two amorphous phases and proof that phase separation was occurring. It was hoped to find similarity with the sodium-boro-silicate system and evidence of the suitability of ionomer glasses as a microporous glass. SEM analysis of glass 1 is shown in Figs 8 and 9.

From Figs 8 and 9, a number of sparse droplets, ranging in size between approximately 20 nm and 100 nm can be seen. The background to the droplets has a speckled appearance and it is unclear why this is so and if there may be some type of phase separated structure here also. While the SEM evidence mainly pointed to a

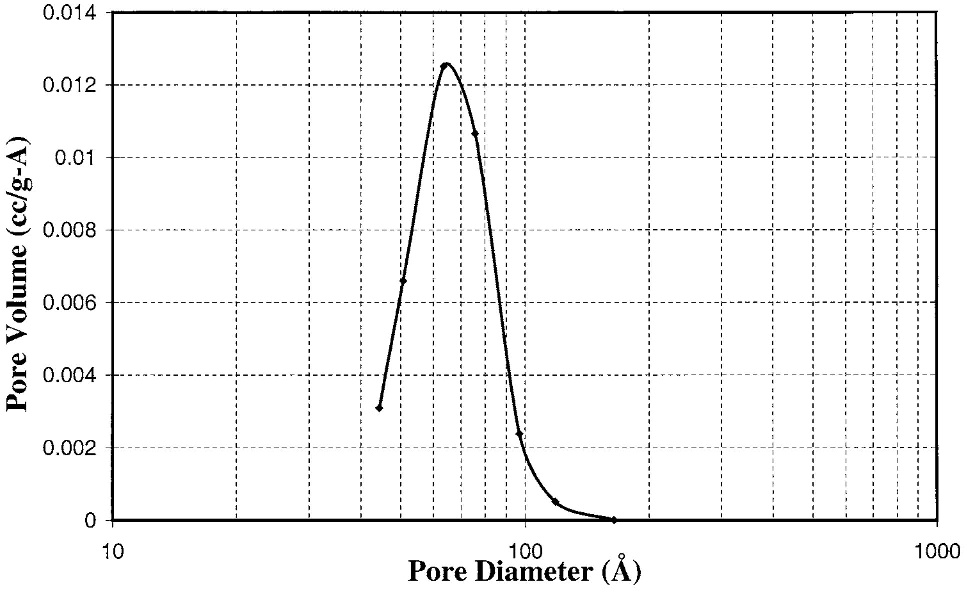

Figure 6 Pore distribution for sample A3.

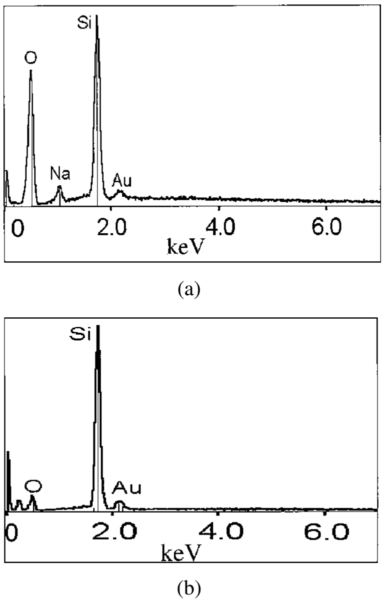

(a)

(b)

Figure 7 EDX spectrum of sodium-boro-silicate glass: (a) before and (b) after leaching.

nucleation and growth mechanism, the areas surrounding the droplets appear speckled and it is unclear as to whether a separate spinodal decomposition mechanism could be occurring here also, perhaps resulting in a very fine scale interconnected structure. Hill *et al.* [11] in a previous SEM study found evidence of an interconnected structure in ionomer glasses heated just past the glass transition. Glass 2 exhibited a similar type of microstructure to glass 1, with sparse droplets distributed in a speckled matrix. However, glass 3 revealed more distinctive features, as shown in Fig. 10.

Scanning electron microscopy of glass 3 confirms that this glass has a very large volume fraction of droplets. While this glass has been heated up to 50°C below its first peak crystallisation temperature (T_p1–50°C) it does show a much greater volume fraction of droplets than glasses 1 and 2 heated to T_p1–50°C. From Table I it can be seen that Glass 3 possesses the structural unit of the crystalline phase, ($Ca/P = 1.67$) and although disordered, the degree of movement and structural rearrangement required for crystallisation should be lower than for the other glasses.

Leaching experiments were conducted on the ionomer glasses. Different concentrations of NaOH solutions were used. Other leachants that were experimented with included 0.3 M HNO_3, 0.3 M HCl, 3 M acetic acid and distilled H_2O. A large number of leaching experiments were conducted. A summary of the leaching treatments that were used and the surface area measurements recorded are shown in Table III. All

TABLE III Leaching conditions and BET surface area measurements of the ionomer glass

Glass	Heat treatment	NaOH leach 10%	Water/HCl/HNO_3/CH_3COOH leach	Surface area ($m^2 g^{-1}$)
1A	None	None	None	3.31
1B	None	None	H_2O 6 h @ 97°C	4.6
1C	None	None	0.3 M HNO_3 6 h @ 97°C	3.48
1D	4 h @ 661°C	None	3 M CH_3COOH 6 h @ 97°C	3.6
1E	4 h @ 661°C	None	H_2O 18 h @ 97°C	12.9
1F	4 h @ 661°C	5% NaOH 6 h @ 97°C	H_2O 1 h @ 97°C	6.9
1G	1 h @ 661°C	9 h @ 97°C	None	15.1
1H	None	9 h @ 97°C	H_2O 14 h @ 23°C	31
1I	None	9 h @ 97°C	H_2O 20 h @ 23°C	36.8
1J	4 h @ 661°C	9 h @ 97°C	H_2O 6 h @ 97°C	41.6
1K	1 h @ 661°C	9 h @ 97°C	H_2O 15 h @ 97°C	38.19
1L	1 h @ 661°C	9 h @ 97°C	H_2O 24 h @ 97°C	44.1

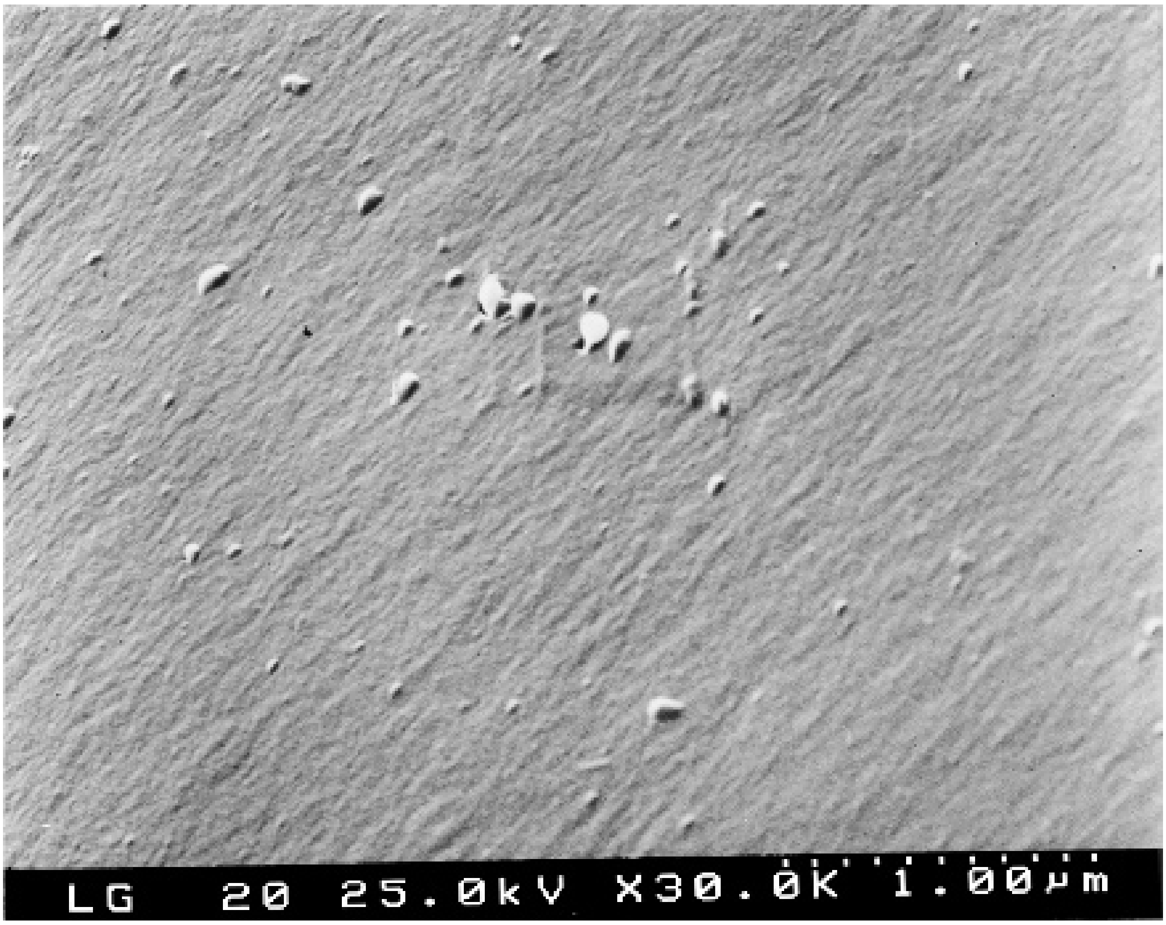

Figure 8 SEM of glass 1 X30K.

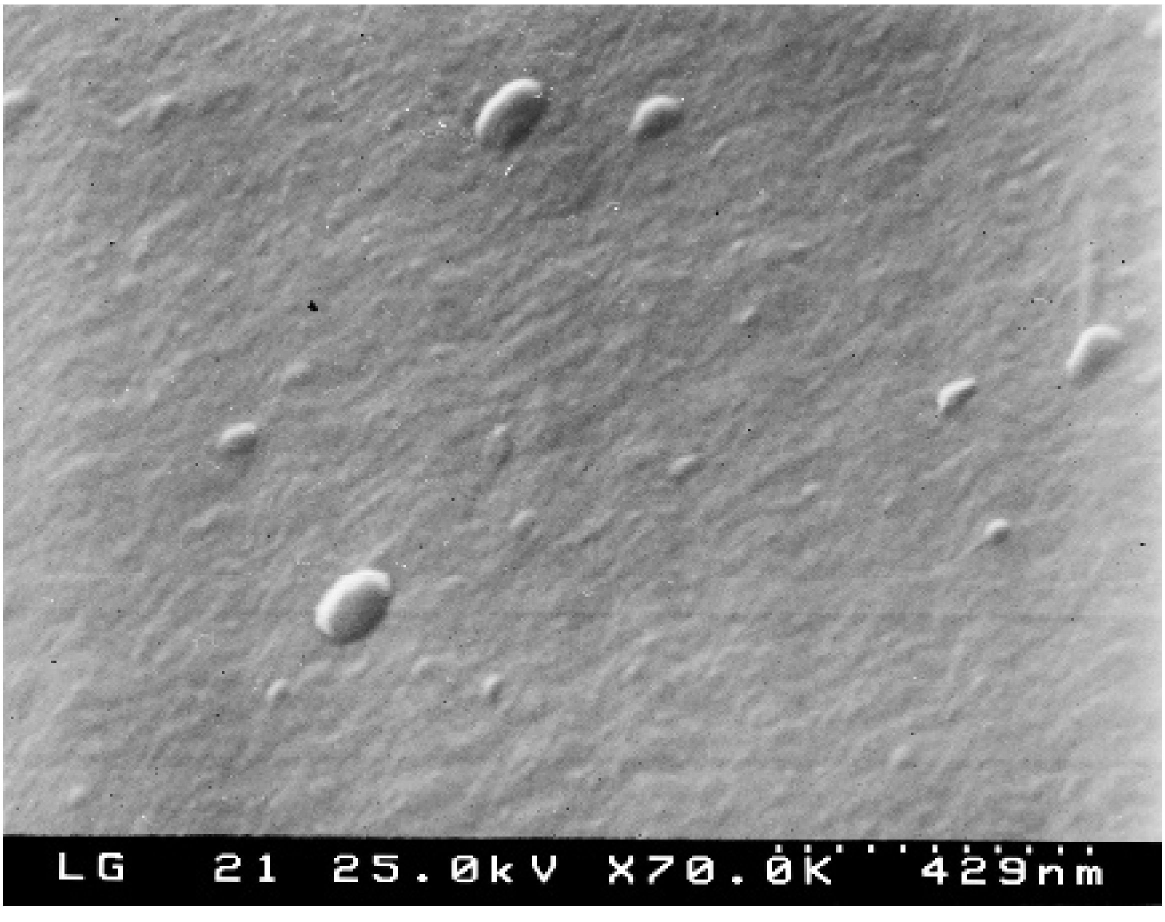

Figure 9 SEM of glass 1 X70K.

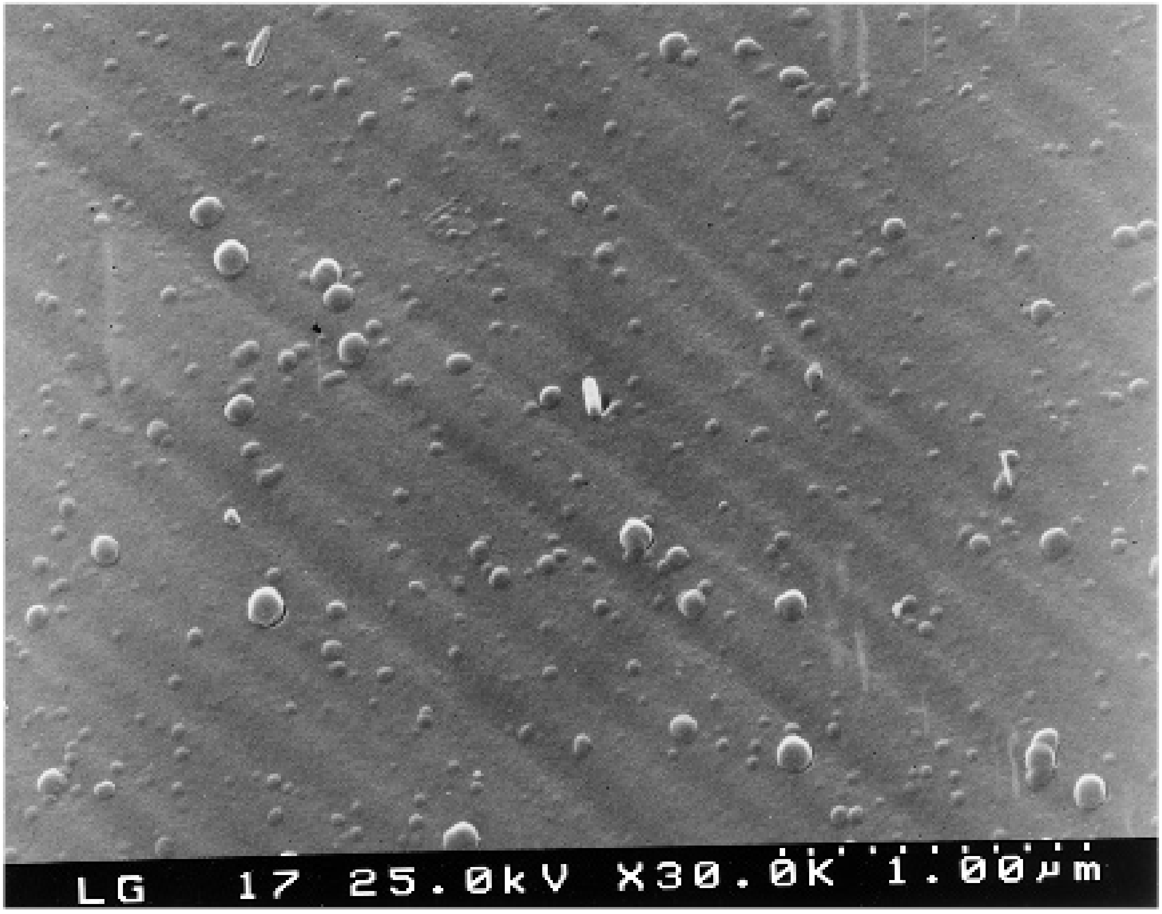

Figure 10 SEM of glass 3, heat-treated to Tp1–50, X30K.

NaOH leaches are 10%, with the exception of glass 1F in which 5% NaOH was used.

The base glass 1A yielded a surface area of 3.3 $m^2\ g^{-1}$. Surprisingly, a 6 h water leach at 97°C only marginally increased the surface area to 4.6 $m^2\ g^{-1}$. Phosphorus is known to be released from glass polyalkenoate cements [29, 30] and glasses with high phosphate contents may be soluble in water; for this reason ionomer glasses have been etched in water prior to transmission electron microscopy analysis [15]. An 18 h leach at 97°C of a quantity of heat-treated glass resulted in a surface area of 12.9 $m^2\ g^{-1}$, but leaching for longer times in water did not result in any further increases in surface area. Nitric acid and acetic acid leaches failed to significantly increase the surface area measurement above that of the base glass. Earlier, from nitric acid etching of SEM samples it was found that HNO_3 had the effect of removing the Al-Si glass matrix. NaOH leaching proved more successful with a surface area of 44.1 $m^2\ g^{-1}$ being the highest value recorded for glass 1L. It is believed that NaOH removes the calcium-phosphate rich phases. It was found that water leaching following an NaOH leach caused the surface area to increase. However, water leaching beyond 24 h did not cause any further increases in the surface area. Pre-heat-treating the glass at a pre-determined optimum nucleation temperature [31] of 661°C did not have a significant bearing on the surface area findings. Leaching experiments on ionomer glasses 2 and 3 showed similar trends to those for glass 1 but no increase above 44.1 $m^2\ g^{-1}$ was recorded. This result was somewhat anomalous, in light of the microstructural differences observed for glass 3 compared to the other glasses.

EDX of the base glass 1A was conducted. See Fig. 11a. As expected, large peaks were detected for aluminium, silicon, calcium and phosphorus with two smaller peaks corresponding to oxygen and fluorine. Fig. 11b is the EDX spectrum for the leached glass 1I. It can be seen that the phosphorus and calcium peaks

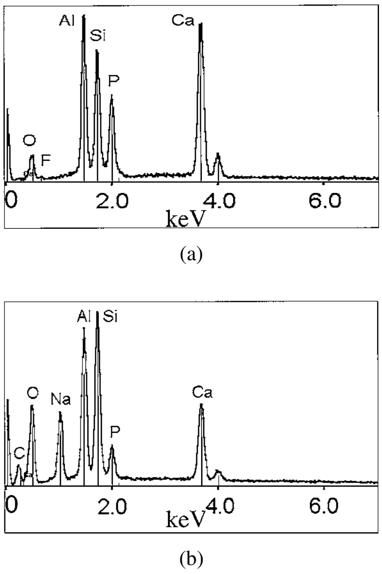

(a)

(b)

Figure 11 EDX spectrums of (a) ionomer glass 1A, and (b) ionomer glass 1I.

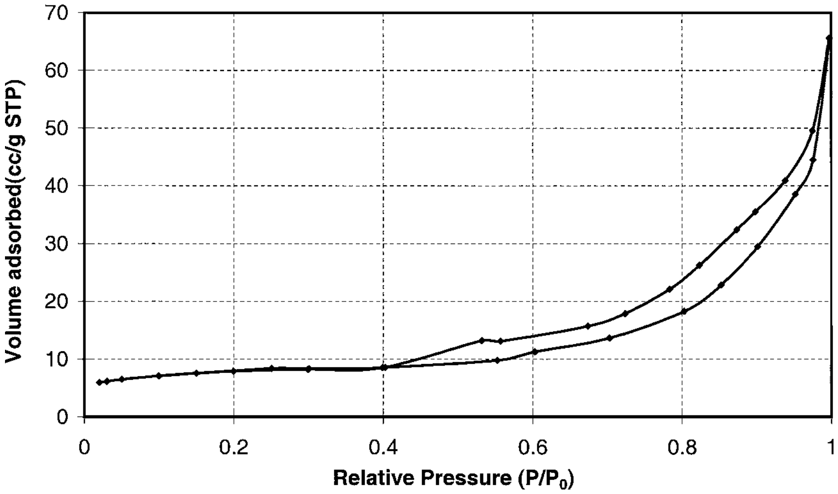

Figure 12 Adsorption-desorption isotherm for glass 1I.

have greatly diminished, the fluorine has disappeared and the silicon and aluminium peaks dominate.

This supports the belief that it is a calcium-phosphate rich phase that is being leached out, but this is not being leached out to completion. However, an aluminium-silicon rich glass phase remains on leaching and this shows a 14-fold increase in surface area over the base glass. An adsorption-desorption analysis of the base glass 1A didn't produce any data, indicating that this glass is completely non-porous. Fig. 12 shows the adsorption-desorption isotherm of glass 1I, which appears to be a Type 4.

This isotherm is almost identical to that observed for the sodium-boro-silicate (A2) sample, but hysterisis is occurring at lower P/P_0 values (<0.6), indicating the presence of smaller pores.

Pore size distribution analyses were conducted on a number of the leached glass 1 samples with high surface areas. The pore distribution for glass 1I is shown in Fig. 13.

A pore distribution with a range of pore sizes between approximately 4 and 11 nm is observed. These pores are smaller than the droplets observed in this glass by SEM, which ranged in size from approximately 20 to 100 nm. This adds some weight to the theory that the calcium-phosphate droplets are not being etched out to completion.

The adsorption-desorption results for the ionomer glass are interesting and represent an alternative indirect method of investigating APS in this glass system. While the leaching process is causing the surface area to increase, it remains unclear whether the droplets are being leached out, or whether there is an interconnected structure, which is not being detected by scanning electron microscopy. Also, stresses generated during leaching can lead to an increase in surface area by causing the glass to break up and form agglomerates. It is a fact that problems were encountered with the Vycor$^{\text{TM}}$ process, including a tendency towards fracture during leaching [32]. It was found that when a phase-separated glass is leached, stresses develop from at least four sources including capillary stresses associated with the high interfacial area produced by phase separation, with excessive strain leading to fracture

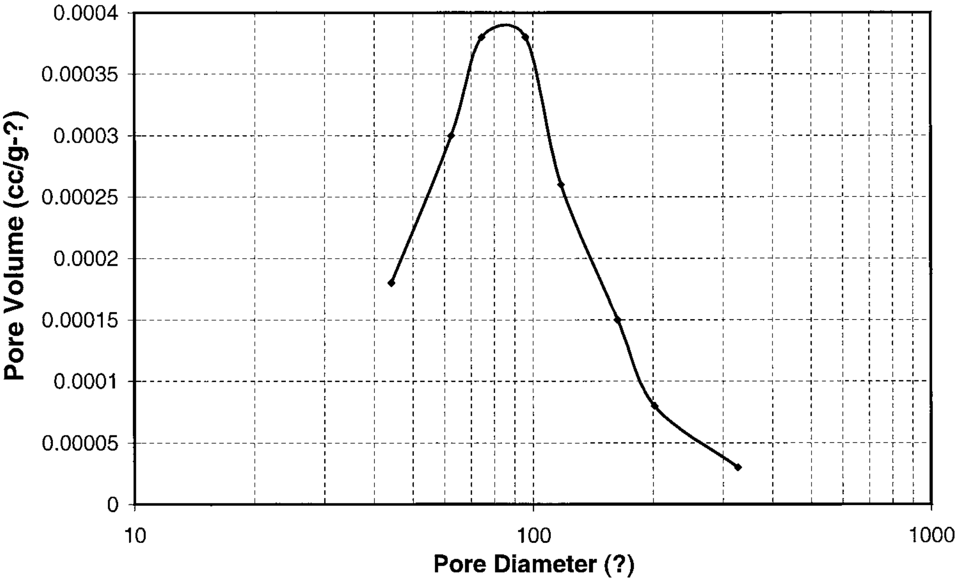

Figure 13 Pore distribution for glass 1I.

following leaching. The 15-fold increase in surface area observed here after leaching would not appear to be as a result of droplets being leached out as this would not result in a substantial increase in surface area, and points more towards the presence of an interconnected structure.

4. Conclusions

The sodium-boro-silicate glass exhibited a classic interconnected structure with a continuous phase present when examined using SEM. The sodium-boro-silicate glass can be leached with a HNO_3solution to remove the sodium-borate phase, resulting in an interconnected porous silica-rich structure. BET surface area analysis and pore distribution analysis showed the base glass to be non-porous ($\sim$9 m^2 g^{-1}), while the leached base glass ($\sim$334 m^2 g^{-1}) exhibited a 40-fold increase in surface area and demonstrated a Type 4 isotherm, indicative of mesoporous materials. A prior heat-treatment of the base glass causes the sodium-borate phase to coarsen and after leaching a 7-fold increase in surface area ($\sim$62 m^2 g^{-1}) over the base glass is observed. This glass also demonstrates a Type 4 isotherm but hysterisis occurs at higher relative pressures indicative of larger pores being present than for the leached base glass. A pore size distribution showed the pores to be in the 4–30 nm range compared to 4–10 nm for the leached base glass. EDX analysis shows the glass to be silica rich after leaching.

Scanning electron microscopy of the ionomer glasses showed the presence of sparse droplets (20–100 nm) dispersed in a matrix. The second phase droplets were spherical with clear interfaces, having no visible connectivity and a random distribution, suggesting a separation mechanism involving nucleation and growth. The background between the droplets had a speckled appearance but it was unclear from SEM alone whether an interconnected structure could also be present. James [33], in a review of APS in inorganic glasses postulates that for some glass systems the effective spinodal boundary may be depressed to lower temperatures and samples would always have to traverse a nucleation region before reaching the spinodal. It may be that the droplets observed are formed on traversing the metastable gap between the spinodal and binodal, whilst the speckled background is due to fine scale APS occurring within the spinodal.

Ionomer base glasses had surface areas of approximately $\sim$3 m^2 g^{-1} and were non-porous. The ionomer glass could be leached in NaOH solution and then water to become reduced in calcium and phosphate and show up to a 15-fold increase in surface area (44 m^2 g^{-1}). Further leaching times however, did not result in a further increase in surface area above 44 m^2 g^{-1}. Adsorption-desorption and pore distribution analysis was conducted on an ionomer glass and revealed a Type 4 isotherm with a pore distribution in the $\sim$6–12 nm range. Prior heat-treatment of the ionomer glasses had no real effect on the surface area measurements. This was in contrast to the sodium-boro-silicate glasses where a heat-treatment could affect an increase in pore size and a corresponding increase in surface area.

Further work is required to investigate the structure of the phase separated ionomer glasses. The 15-fold increase in surface area observed on leaching these glasses implies that an interconnected structure may be present. The leaching of a microstructure consisting of discrete droplets dispersed in a matrix would not lead to a substantial increase in surface area. Furthermore, from scanning electron micrographs there is evidence of some type of structure, possibly a fine-scale interconnected structure existing in tandem with a droplet microstructure. Small angle X-ray scattering (SAXS) has long been recognised as the most powerful method for investigating the early stage kinetics in the unstable spinodal region, and this could probably be employed to determine the existence of an interconnected morphology in the ionomer glasses.

Acknowledgements

The authors would like to gratefully acknowledge the support of Brite EuRam Contract BRPR-CT96-0230. The authors would like to offer thanks to Dr. Seamus McMonagle for his generosity with the BET instrument. Finally the authors would like to thank Dr. Rui N. Correia for his help with the FESEM instrument.

References

1. J. HAMMEL and T. ALLERSMO, "Phase Separatable Borosilicate Glass Compositions," US Patent, No. 3,972,720 (Aug. 3, 1976).
2. T. H. ELMER, in "Engineered Materials Handbook," Vol. 4 (ASM International, USA, 1991) p. 427.
3. N. FORD and R. TODHUNTER, in "Glasses and Glass Ceramics" (Chapman and Hall, 1989).
4. W. HALLER and P. B. MACEDO, *Phys. Chem. Glasses* **5** (1968) 153.
5. J. W. CAHN and R. J. CHARLES, *ibid.* **6** (1965) 181.
6. A. PAUL, in "Chemistry of Glass" (Chapman & Hall, London, 1982).
7. T. H. ELMER, *Amer. Ceram. Soc. Bull.* **59** (1980) 525.
8. J. B. CLARK, M. A. RES and S. HART, *Glastech. Ber.* **57** (1984) 269.
9. T. H. ELMER and T. P. SEWARD, *ibid.* **64** (1991) 66.
10. K. EGUCHI, H. TANAKA, T. YAZAWA and T. YAMNGURO, "Chemically Durable Porous Glass and Process for the Manufacture Thereof," US Patent, No. 4,778,777 (Oct. 18, 1988).
11. R. G. HILL, C. GOAT and D. WOOD, *J. Amer. Ceram. Soc.* **75** (1992) 778.
12. *Idem.*, *ibid.* **75** (1992) 778.
13. A. CLIFFORD and R. HILL, *J. Non. Cryst. Solids.* **196** (1996) 346.
14. E. A. WASSON and J. W. NICHOLSON, *Brit. Poly. J.* **23** (1990) 179.
15. C. JANA and W. HÖLAND, *Silicates Industriels* **56** (1991) 215.
16. T. I. BARRY, D. J. CLINTON, L. A. LAY and R. P. MILLER, ASPA Dental Cement NPL Report Part 1 (1972) p. 1.
17. C. MOISESCU, C. JANA and C. R ÜSSEL, *J. Non. Cryst. Solids.* **248** (1999) 169.
18. A. RAFFERTY, R. HILL and D. WOOD, *J. Mater. Sci.* **35** (2000) p. 1.
19. A. RAFFERTY, R. G. HILL and D. WOOD, *J. Mater. Sci.* **38**(11) (2003) 2311.
20. Z. STRNAD, "Glass-Ceramic Materials" (Elsevier Science Publishing Company Inc. Amsterdam, 1986).
21. W. HALLER and P. B. MACEDO, *Phys. Chem. Glasses* **5** (1968) 153.
22. J. W. CAHN and R. J. CHARLES, *ibid.* **6** (1965) 181.
23. J. W. CAHN and J. E. HILLIARD, *J. Chem. Phys.* **28** (1958) 258.
24. O. V. MAZURIN, *Phys. Chem. Glasses* **9** (1968) 165.

25. S. J. GREEG and K. S. SING, “Adsorption, Surface Area and Porosity” (Academic Press, London and New York, 1967).
26. S. BRUNAUER, L. S. DEMING, W. S. DEMING and E. J. TELLER, *J. Amer. Ceram. Soc.* **62** (1940) 1723.
27. M. M. DUBININ, *Zhur. Phys. Chem.* **34** (1960) 959.
28. S. STORCK, H. BRETINGER and W. F. MAIER, *Appl. Catal. A: General* **174** (1998) 137.
29. H. J. PROSSER, D. R. POWIS and A. D. WILSON, *J. Dent. Res.* **65** (1986) 146.
30. S. CRISP and A. D. WILSON, *ibid.* **53** (1974) 1420.
31. A. MARROTTA, A. BURI, F. BRANDA and S. SAIELLO, “Advances in Ceramics” (The American Ceramic Society, Inc., 1982) vol. 4, p. 146.
32. G. W. SCHERER and M. G. DREXHAGE, *J. Amer. Ceram. Soc.* **68** (1985) 419.
33. P. F. JAMES, “Glasses and Glass-Ceramics” (Chapman and Hall, London, 1989).

Received 4 April
and accepted 7 July 2003